Eur. Phys. J. D **9**, 35–39 (1999)

THE EUROPEAN PHYSICAL JOURNAL D

EDP Sciences
© Società Italiana di Fisica
Springer-Verlag 1999

The reactivity of gold and platinum metals in their cluster phase

U. Heiz, A. Sanchez, S. Abbet, and W.-D. Schneider

Université de Lausanne, Institut de Physique de la Matière Condensée, CH-1015 Lausanne, Switzerland

Received: 2 September 1998 / Received in final form: 27 October 1998

Abstract. Platinum surfaces are known to be among the most active ones for the oxidation of carbon monoxide, whereas gold surfaces are completely inert for this reaction. The question remains: Do small clusters of these two metals maintain these distinct differences? To answer this question, we have employed temperature-programmed reaction (TPR) and Fourier transform infrared (FTIR) spectroscopy to investigate the reactivity of small platinum and gold clusters consisting of up to 20 atoms. These clusters are generated in the gas phase by a laser evaporation source and, after mass selection, are deposited with low kinetic energy onto thin MgO films. The oxidation of CO is studied for the octamer and the icosamer under UHV conditions. Surprisingly, all investigated cluster sizes are catalytically active. Pt_{20} shows the highest reactivity and oxidizes almost 6 CO molecules, whereas Pt_8, Au_{20}, and Au_8 oxidize just one CO molecule under identical experimental conditions.

PACS. 36.40.Jn Reactivity of clusters – 82.65.Jv Heterogeneous catalysis at surfaces – 82.80.Ch Ultraviolet, visible, infrared, Raman, microwave, and magnetic resonance spectroscopic analysis methods, spectrophotometry; colorimetry

1 Introduction

The active components in the control of automotive pollution are small platinum, palladium, and rhodium particles supported on oxide surfaces. Here the catalytic oxidation of carbon monoxide is one of the most important steps in a technology costing the American consumer about five billion dollars per year [25]. The huge number of studies found in the literature dealing with this reaction (almost three publications a day in 1997) reflects the effort to understand this catalytic process. The conversion of CO and O_2 into CO_2 in the gas phase has a free enthalpy of $-280\,\mathrm{kJ/mol}$ and is therefore thermodynamically allowed. However, in order to initiate this reaction, the activation energy for the dissociation of O_2 has to be overcome, and it is the task of the catalyst to reduce this energy. Studies on single crystals, on supported particles as well as on real catalysts have revealed many details about this catalytic process. On highly coordinated Pt atoms, e.g., a Pt(111) single crystal, carbon monoxide can be oxidized at low temperature (160 K) [1, 18, 20]. In this case, oxygen atoms that are produced during the dissociation process of O_2 on the surface, oxidize carbon monoxide. In such a mechanism, oxygen atoms react with CO before they reach the energy minimum of the oxygen–surface interaction potential, and therefore no additional activation for the actual oxidation step is needed [1]. A second reaction channel on Pt(111) involves chemisorbed oxygen atoms, which oxidize adsorbed CO at temperatures higher than 200 K. This mechanism can also be observed on low coordinated platinum sites, e.g., the ones on a Pt(355) surface [24, 28], and the oxidation temperature of this mechanism is sensibly dependent on the character of the reactive site [28]. In addition to this rather detailed picture of the energetics of the process, a complex spatial and temporal pattern of this seemingly simple reaction was discovered [5]. Studies on Pt(100) and Pt(110) surfaces revealed a complicated modification of the overall CO oxidation caused by an adsorption-induced change in the surface structure, which leads to oscillations during the reaction [21].

Real catalysts for the oxidation of CO consist of highly dispersed metal particles on refractory metal oxides [6–8]. Besides changes in the reactivity due to the existence of different crystalline facets on particles a few nanometers in size [4, 16], pronounced size effects in the catalytic behavior of very small clusters consisting of only a few atoms should be apparent [11, 13]. This is caused by the changing coordination number in different geometric structures and/or the change in electronic structure as a function of cluster size. Such a size-dependent variation of the chemical properties was observed in several gas-phase studies, where reactivities of small metal clusters were investigated. Bérces, et al. have measured absolute rate coefficients for the reaction of Nb_n clusters ($n = 2 - 20$) with H_2 and N_2 at different temperatures [2], confirming the low reactivities of Nb_8, Nb_{10}, and Nb_{16} measured in earlier experiments [19, 30]. They recognized an anticorrelation of the reactivity with an effective ionization potential of the cluster that includes

the polarization of the charge on the cluster cation. Consequently, reactivities of such small clusters are directly related to their intrinsic electronic properties. This correlation between the electronic structure and the reactivities of niobium clusters has also been observed experimentally by Kietzmann *et al.* [17] These authors estimated the HOMO–LUMO gap from photoelectron spectra and observed closed shells and a large HOMO–LUMO gap for the unreactive cluster sizes. In addition, Bérces *et al.* [2] have observed clearly biexponential kinetic plots, indicative of the presence of different isomers with distinct reactivities. They suggest that, in addition to electronic effects, steric effects also play a decisive role in determining cluster reactivities [2]. Shi *et al.* have even investigated a whole catalytic cycle and studied the catalytic oxidation of CO on free platinum clusters in a molecular beam experiment [23].

In this work we have gone a step further towards real catalysts by depositing small gas-phase clusters on an oxide surface and studying a complete chemical reaction, the oxidation of CO as a function of the precise number of atoms in the clusters [12, 14]. We chose platinum and gold clusters in order to answer the question of whether small clusters consisting of only a few atoms, and supported on an oxide surface, are already catalytically active. In contrast to platinum, gold is known to be the least reactive noble metal [9], and extended Au surfaces neither chemisorb CO nor oxidize this molecule in the presence of molecular oxygen. Gold catalysts prepared by precipitation oxidize CO at low temperature [3], but only hints about the active cluster size are given in this work. In the present investigation, we compare the reactivity of the two systems, hoping to get insights into whether the different catalytic properties and the underlying concepts are also valid for model catalysts consisting of such small nanostructures.

2 Experiments

The clusters are generated in a recently developed high-frequency laser evaporation source, which is described in detail elsewhere [15]. A 100 Hz Nd:YAG laser is focused onto a target, which is mounted on a motor-driven hypocycloidal planetary gear assembly. The produced plasma then expands into the source cavity, which consists of a thermalization chamber and an exchangeable expansion nozzle. Unlike other laser evaporation sources, the cavity and expansion nozzle are coaxial with respect to the incoming laser beam. This increases the cluster flux because, first, cluster losses due to extended wall deposits are reduced, and, second, the absence of an additional laser channel decreases the leakage rate of He. The produced cluster ions are then transported by ion optics through differentially pumped vacuum chambers, are mass-selected by a quadrupole mass spectrometer, and, finally, are focused onto an appropriate substrate. With this experimental setup, depending on cluster material and cluster size, it is possible to produce hundreds of picoamperes up to a couple of nanoamperes of size-selected cluster ions. In addition, since the clusters are produced by an adiabatic or supersonic expansion, they show relatively narrow kinetic energy profiles (0.2–2 eV) allowing for the deposit of clusters with low energy (< 0.2 eV/atom).

In these experiments, thin MgO(100) films are grown on Mo(100) surfaces by evaporating Mg in an oxygen background using a well-established recipe [27]. The quality of these films was ensured in depth by Auger electron spectroscopy (AES), temperature-programmed desorption (TPD), Fourier transform infrared (FTIR) spectroscopy, high-resolution electron energy loss spectroscopy (HREELS), X-ray photoelectron spectroscopy (XPS), UV photoelectron spectroscopy (UPS) and low-energy electron diffraction (LEED) indicating clean surfaces with bulk-like properties [10, 15, 22].

The catalytic properties of the size-selected, supported clusters are analyzed in a UHV chamber with a base pressure better than 1×10^{-10} Torr. It is equipped with a FTIR spectrometer in single reflection mode, a hemispherical electron analyzer for AES and a mass spectrometer for temperature-programmed desorption (TPD) and reaction (TPR) studies. For the reaction studies, the supported clusters are exposed to the reactants by a calibrated molecular beam doser [26].

For the presented experiments, isotopically labeled $^{18}O_2$ is used in order to unambiguously attribute the CO_2 production to the clusters. For the oxidation experiments on gold clusters, ^{13}CO is used, giving a slightly better signal-to-noise ratio. All deposited monodispersed clusters are first exposed to the same number of oxygen molecules (20 O_2 per deposited atom) at 90 K. Subsequently, the clusters are exposed to the same number of CO molecules and, finally, as a function of the temperature, the catalytically formed $^{12}C^{16}O^{18}O$ and $^{13}C^{16}O^{18}O$ are monitored by the mass spectrometer for the platinum and gold clusters, respectively.

3 Results and discussion

3.1 Oxidation of CO on Pt_{20} and Pt_8 deposited on MgO(100)

Figure 1 shows TPR spectra of $^{12}C^{16}O^{18}O$ and $^{12}C^{16}O$ for the CO oxidation on Pt_{20} and the evolution of the vibrational frequency of the adsorbed CO during the reaction as a function of temperature. Remarkably, on such small metal particles consisting of only 20 atoms, CO_2 is already readily produced. The CO oxidation on Pt_{20} occurs at three different temperatures, 120 K, 310 K, and 470 K, labeled α, β_1, and β_2. By integrating the total area of the TPR spectra, the total number of produced CO_2 molecules per cluster can be obtained. For this evaluation, we calibrated our mass spectrometer by measuring the well-known amount of CO desorbing from a Mo(100) single crystal [29] and taking into account the different ionization cross sections for CO and CO_2. The number of deposited clusters is obtained by integrating the ion current during deposition. With this method, the number of

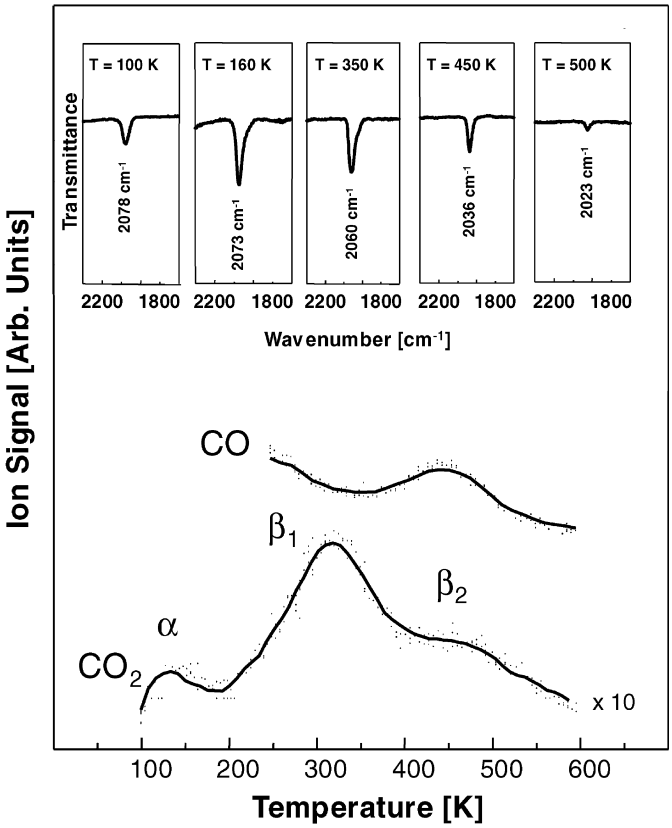

Fig. 1. Temperature-programmed reaction (TPR). CO_2 production and CO desorption for Pt_{20} as function of temperature. Dots: data; full line: data smoothing with adjacent averaging (25 points). Isotopically labeled $^{12}C^{16}O$ and $^{18}O_2$ are used to unambiguously attribute the catalytic activity to the supported clusters. The number of desorbing molecules can be estimated by integrating the TPR spectra (see text). Inset: FTIR spectra of CO adsorbed during the catalytic oxidation (e.g., coadsorbed with O_2) are shown. The samples are annealed to the indicated temperatures, and all spectra are then recorded at 90 K.

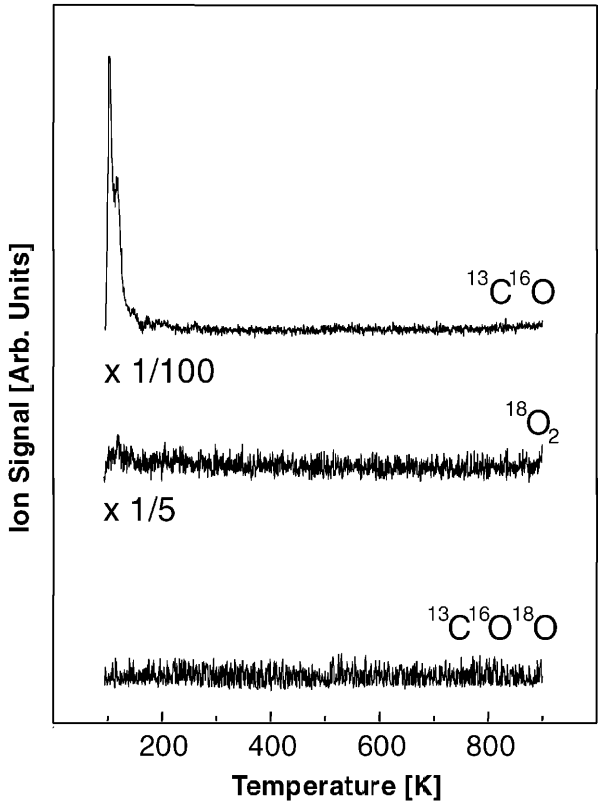

Fig. 2. TPR spectra of $^{13}C^{16}O^{18}O$, $^{18}O_2$, and $^{13}C^{16}O$ after a clean $Mg^{16}O(100)$ film is exposed to the same amount of $^{13}C^{16}O$ and $^{18}O_2$, as for the cluster experiments. Note that no carbon dioxide is formed on these films (bottom). Carbon monoxide (top) and a small amount of molecular oxygen (middle) physisorbs on MgO(100) at low temperature. In a separate experiment, a clean $Mg^{18}O(100)$ film was exposed to $^{13}C^{16}O$ and $^{16}O_2$; no $^{13}C^{16}O^{18}O$ was detected, possibly because of an exchange reaction with the substrate (result not shown).

catalytically produced CO_2 is 5.7 ± 0.1 for deposited Pt_{20}. In addition to CO_2, CO desorbs from the cluster at around 450 K. Therefore, the oxidation of CO on this cluster size is not stoichometric under the chosen experimental conditions. In addition to these TPR studies, the vibrational frequency of adsorbed CO on the cluster is monitored during the reaction (see inset of Fig. 1). Prior to oxidation, at 100 K, one type of coadsorbed CO is detected, revealing an absorption frequency of 2078 cm^{-1}. Up to 160 K, this frequency redshifts (2073 cm^{-1}) and gains intensity due to either the desorption of molecular adsorbed oxygen from the cluster and subsequent migration of physisorbed CO towards the cluster, or a possible reorientation of the adsorbed CO molecules, which may result in an enhanced absorption cross section. With increasing temperature, the band further redshifts (2060–2023 cm^{-1}) and finally disappears at temperatures above 500 K in accordance with the CO oxidation and the observed desorption of CO.

The same experiment is repeated, but this time Pt_{20} is deposited on $Mg_{18}O$ and exposed to $^{16}O_2$ and $^{12}C^{16}O$. A possible detection of $^{12}C^{16}O^{18}O$ points unambiguously to an oxidation of CO at the cluster–oxide interface. The TPR spectrum (not shown) shows two small peaks at 280 K, and 480 K, indicating the existence of two different oxidation mechanisms at the cluster–support interface. In contrast, at the same experimental conditions, clean oxide films do not catalyze the oxidation of CO, but physisorb carbon monoxide and a small amount of oxygen (Fig. 2).

The oxidation of CO is compared in Fig. 3 for Pt_8 and Pt_{20}, showing distinct differences. The smaller cluster size is clearly less reactive, and oxidizes only one CO molecule at a temperature of around 300 K. On Pt_{20}, a total number of 5.7 ± 0.1 CO_2 molecules is produced per cluster at reaction temperatures of 120 K, 320 K, and 470 K. These different shapes of the two TPR spectra, shown in Fig. 3, point to a different number of reactive sites on each cluster. Reactive sites for both cluster sizes are characterized by measuring the vibrational frequencies of the probe molecule CO adsorbed on the clean cluster surface. After exposing Pt_8 to CO, only one vibrational band at 2065 cm^{-1} is observed, whereas for Pt_{20}, frequen-

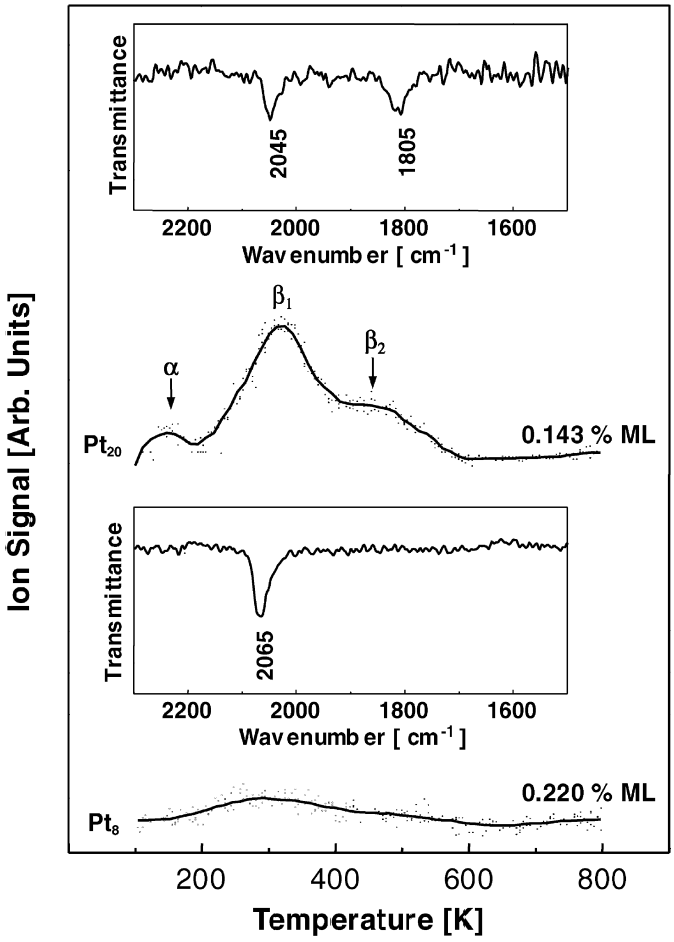

Fig. 3. TPR: CO_2 production as a function of the temperatures for Pt_8 and Pt_{20}. Cluster coverages are given as the percentage of a monolayer (ML), with 100% ML corresponding to 2.2×10^{-15} clusters/cm^{-2}. Inset: FTIR spectra of CO adsorbed on the clean, supported clusters (spectra taken at 90 K).

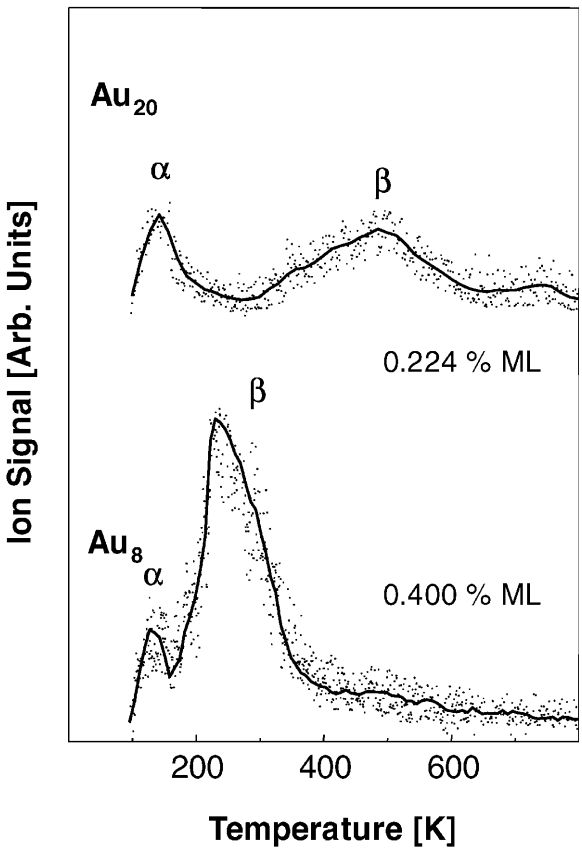

Fig. 4. TPR: CO_2 production on Au_8 and Au_{20} as a function of temperature. Dots: data; full line: data smoothing with adjacent averaging (40 points). Isotopically labeled $^{13}C^{16}O$ and $^{18}O_2$ are used to unambiguously attribute the catalytic activity to the supported clusters and to increase the signal-to-noise ratio. Cluster coverages are given as percentage of a monolayer (ML), with 100% ML corresponding to 2.2×10^{-15} clusters/cm^{-2}.

cies at 2045 cm^{-1} and 1805 cm^{-1} are detected, pointing towards two different adsorption sites. Note that the vibrational frequencies of CO adsorbed on the clean surface of Pt_{20} (2045 cm^{-1} and 1805 cm^{-1}) differ from the one adsorbed during the oxidation reaction (2078–2023 cm^{-1}). In the latter case, adsorption sites of the clusters are occupied by adsorbed oxygen, and the changed chemical interaction of the oxidized cluster with CO alters the vibrational frequency of the adsorbed CO, in comparison to the clean cluster.

The low temperature CO oxidation on Pt_{20}, labeled α, affirms low activation energy for the formation of CO_2. As in the single-crystal studies, we therefore attribute the following mechanism to the α state: At low temperatures (100 K), oxygen adsorbs molecularly on certain adsorption sites of Pt_{20}. When the cluster is heated, two possible reaction channels exist: First, oxygen may desorb from the cluster, and second, the thermal energy may be sufficient to overcome the activation energy for O_2 dissociation. In the latter case, the trapped oxygen atom reacts with adjacent CO before it reaches the energy minimum of the interaction potential of adsorbed O on Pt_{20} [1, 20]. The high-temperature CO oxidation (β) occurs after oxygen molecules are dissociated by the cluster. Adsorbed O atoms then oxidize CO, where the different oxidation temperatures characterize the activation energies for the reaction,

$$\mathrm{O(ad)} + \mathrm{CO(ad)} \rightarrow \mathrm{CO_2}$$

and sensibly depend on the active site of the cluster. We further note that the oxidation is blocked when the cluster is exposed first to CO and then to O_2.

3.2 Oxidation of CO on Au_{20} and Au_8 deposited on MgO(100)

In Fig. 4, the TPR spectra of $^{13}C^{16}O^{18}O$ during the oxidation of CO on Au_{20} and Au_8 are shown. Surprisingly, carbon monoxide is oxidized on small gold clusters also, at temperatures around 140 K (α mechanism) and at temperatures above 200 K (β mechanism). The spectra reveal clear differences between the two cluster sizes. In

the β mechanism, Au_{20} oxidizes CO at 500 K, whereas Au_8 is most reactive at 240 K, suggesting higher activation energy for Au_{20}. This may be explained by a stronger cluster–oxygen interaction in the case of Au_{20}. These results clearly show that gold becomes reactive when going to small clusters, in contrast to the distinct nobleness of gold in the bulk limit.

In comparison to Pt_{20}, which catalytically oxidizes about 6 CO molecules, the reactivity of Au_{20} (1 CO per cluster) is considerably smaller. The octamers of both metals show similar activities (~ 1 CO per cluster). As shown by Hammer and Nørskov [9], the low reactivity or nobleness of gold is basically related to two factors: the degree of filling of the antibonding states on adsorption of a molecule, and the degree of orbital overlap with this adsorbate. These two factors determine the strength of the adsorbate–metal interaction and the energy for dissociation, in our case the dissociation of oxygen. Using density functional theory (DFT), Hammer and Nørskov point out that the nobleness of gold can be explained by the different coupling of the adsorbant's states with the d band of gold. As long as this coupling is not strong enough to push the antibonding state above the Fermi level of the metal upon adsorption, there is an additional repulsive interaction, which is responsible for the nobleness of gold. Our results show that oxygen is adsorbed and dissociated on small gold clusters and that this antibonding state is therefore pushed slightly above the Fermi level of the cluster. Interestingly, the lower reactivity of Au_{20} in comparison to Pt_{20} indicate that the different chemical properties observed for the bulk surfaces start to manifest themselves already for these cluster sizes.

4 Conclusions

Using gas-phase clusters and depositing them with low energies on well-characterized oxide surfaces, model catalysts can be obtained, which are ideal for studying size effects in catalytic reactions. We have shown that small Pt clusters containing of up to 20 atoms are already active for the oxidation of CO. In addition, we observed distinct size effects when comparing Pt_8 with Pt_{20}. More surprisingly, we observed that small gold clusters are also catalytically active, in contrast to the nobleness of gold single crystals. In addition, the much smaller reactivity of Au_{20} in comparison to Pt_{20} already points to the different chemical properties of both metal surfaces. In the future, the variation of the sticking probability of the two molecules involved in the catalytic reaction will be measured as a function of cluster size, in order to disentangle the influence of the sticking probability and the conversion efficiency of the adsorbed molecules on the observed catalytic activity. In addition, a larger size range will be studied, towards the development of concepts that govern the catalytic reactivity of small, size-selected clusters on surfaces, and which can eventually be used to tune, on an atom-by-atom basis, the reactivity of such small clusters.

The authors would like to thank the Swiss National Science Foundation for financial support and F. Patthey for fruitful discussions.

References

1. K.-H. Allers, H. Pfnuer, P. Feulner, D.J. Menzel: Chem. Phys. **100**, 3985 (1994)
2. A. Berces, P.A. Hackett, L. Lian, S.A. Mitchell, D.M. Rayner: J. Chem. Phys. **108**, 5476 (1998)
3. D.A.H. Cunningham, W. Vogel, H. Kageyama, S. Tsubota, M. Haruta: J. Catal. **177**, 1 (1998)
4. C. Duriez, C.R. Henry, C. Chapon: Surf. Sci. **253**, 190 (1991)
5. G. Ertl, P.R. Norton, J. Ruestig: Phys. Rev. Lett. **49**, 177 (1982)
6. H.J. Freund: Angew. Chem. Int. Ed. Engl. **36**, 452 (1997)
7. D.W. Goodman: Surf. Rev. Lett. **2**, 9 (1995)
8. D.W. Goodman: Chem. Rev. **95**, 523 (1995)
9. B. Hammer, J.K. Norskov: Nature **376**, 238 (1995)
10. J.-W. He, J.S. Corneille, D.W. Goodman: Appl. Surf. Sci. **72**, 335 (1995)
11. U. Heiz: "Physical and Chemical Properties of size-selected, supported clusters". In: *Recent Res. Devel. in Physical Chem.*, ed. by S.G. Pandalai, Vol. 2 (Transworld Research Network, Trivandrum 1998)
12. U. Heiz, A. Sanchez, S. Abbet, W.-D. Schneider: J. Am. Chem. Soc. **121**, 3214 (1999)
13. U. Heiz, W.-D. Schneider: "Physical Chemistry of Supported Clusters". In: *Metal Clusters and Dots*, ed. by K.-H. Meiwes-Broer (Springer, Heidelberg 1999)
14. U. Heiz, F. Vanolli, A. Sanchez, W.-D. Schneider: J. Am. Chem. Soc. **120**, 9668 (1998)
15. U. Heiz, F. Vanolli, L. Trento, W.-D. Schneider: Rev. Sci. Instrum. **68**, 1986 (1997)
16. C.R. Henry, C. Chapon, C. Duriez: Surf. Sci. **253**, 177 (1991)
17. H. Kietzmann, J. Morenzin, P.S. Bechthold, G. Gantefoer, W. Eberhardt: J. Chem. Phys. **109**, 2275 (1998)
18. T. Matsushima: Surf. Sci. **127**, 403 (1983)
19. M.D. Morse, M.E. Geusic, J.R. Heath, R.E. Smalley: J. Chem. Phys. **83**, 2293 (1985)
20. Y. Ohno, T. Matsushima: Surf. Sci. **241**, 47 (1991)
21. H.H. Rosenmund: Surf. Sci. Rep. **29**, 265 (1997)
22. M.-H. Schaffner, F. Patthey, W.-D. Schneider, L.G.M. Pettersson: Surf. Sci. **450**, 402 (1998)
23. Y. Shi, K.M.J. Ervin: Chem. Phys. **108**, 1757 (1998)
24. A. Szabo, M.A. Henderson, J.T. Yates: J. Chem. Phys. **96**, 6191 (1992)
25. K.C. Taylor: *Automotive Catalytic Converters* (Springer-Verlag, New York 1984)
26. A. Winkler, J.T. Yates: J. Vac. Sci. Technol. A **6**, 2929 (1988)
27. M.C. Wu, J.S. Corneille, C.A. Estrada, J.-W. He, D.W. Goodman: Chem. Phys. Lett. **182**(5), 472 (1991)
28. J. Xu, J.T. Yates: J. Chem. Phys. **99**, 725 (1993)
29. F. Zaera, E. Kollin, J.L. Gland: Chem. Phys. Lett. **121** (4/5), 464 (1985)
30. M.R. Zakin, R.O. Brickman, D.M. Cox, A.J. Kaldor: Chem. Phys. **88**, 3555 (1988)